Electronic Supplementary Material (ESI) for ChemComm.
This journal is © The Royal Society of Chemistry 2018

Neptunium(V)-Mediated Transuranium-Rotaxane Network Incorporating Mechanically-Interlocked [*c*2]Daisy Chain Unit†

Lei Mei‡,[a] Chao Xu‡,[b] Qun-yan Wu,[a] Kong-qiu Hu,[a] Li-yong Yuan,[a] Jing Chen,[b] Cheng-liang Xiao,[c] Shu-ao Wang,[c] Zhi-fang Chai[a, c] and Wei-qun Shi[a]*

Supporting Information

Table of contents

S1. Experimental Procedures 3

Materials.

General Methods.

Synthesis.

X-ray Single Structural Determination.

Computational details

S2. Figures and Tables 6

Figure S1. Optical photograph of yellow-green block crystals of **NRCP-1**: a) yellow-green block crystals for **NRCP-1**, accompanied by a certain amount of colorless crystals for pseudorotaxane carboxylic acid, H_2**L**-ClO_4-1; b) a snapsnot of **NRCP-1**.

Figure S2. Crystal structures of H_2**L-**ClO_4-1 (a) and H_2**L**-ClO_4-2 (b).

Figure S3. Optical photograph of light-yellow block crystals of **UP-107**: a) light-yellow cubic crystals of **UP-107**, accompanied by a certain amount of colorless crystals for pseudorotaxane carboxylic acid, H_2**L**-ClO_4-2; b) a snapsnot of **UP-107**.

Figure S4. The asymmetric unit of **NRCP-1** containing one neptunyl ion, two halves of C6BPCA@CB6 pseudorotaxane ligands, and one coordinated water molecule as well as one crystal lattice water molecule and one perchlorate counter-ion

Figure S5. A unique interwoven neptunium(V)-rotaxane coordination network of **NRCP-1** with two sets of independent but mechanically-interlocked neptunyl-rotaxane layered structures.

Figure S6. The interwoven neptunium(V)-rotaxane coordination network of **NRCP-1** separated into an array of neptunyl-rotaxane one-dimensional chain cross-linked through coordination of exposed carbonyl groups of CB6 coordinating with neptunyl centers from adjacent chains in stick model (a) and space-filling model (b).

Figure S7. a) Interwoven coordination network; b) Interwoven coordination network with all the perchlorate anions fill in pairs in the quadrilateral holes; c) interwoven coordination network viewed from the side-on; d) closely packing of coordination networks in crystal lattice through weak interactions.

Figure S8. a) The crystallographically unique uranyl center with a pentagonal-bipyramid geometry in **UP-107**; b) crystal packing of two-dimensional networks in **UP-107**; c) a two-dimensional polyrotaxane network with rhombic-shaped loops in **UP-107**; d) perchlorate ions in pair trapped in the rhombic-shaped cavity of two-dimensional polyrotaxane network in **UP-107**.

Figure S9. A direct comparison of bond distances between metal ion and oxygen donors in **NRCP-1** (left) and **UP-107** (right).

Figure S10. The simplified model of coordination sphere of neptunyl derived from crystal structure of **NRCP-1**.

Figure S11. Natural bond orbitals of Np-O bonds. The isosurface value of the MOs is established as 0.03 au.

Figure S12. The UV-vis-NIR absorption spectroscopy recorded from crystals of **NRCP-1** using a microspectrophotometer. Insert: optical photograph of yellow-green block crystals of **NRCP-1**.

Table S1. Crystal data and structure refinement for **NRCP-1**, **UP-107**, H_2**L**-ClO_4-1 and H_2**L**-ClO_4-2.

Table S2. Selected bond distances (Å) related to neptunium center in **NRCP-1** and **UP-107**.

Table S3. Products under synthesis conditions from uranium or neptunium sources.

Table S4. Calculated Np-O bond distances (Å) and the electron density (ρ(r), au), and Laplacian ($\nabla^2\rho$(r), au) at the Np-O BCP at the B3LYP/ECP60MWB/6-31G(d) level of theory, and the NM and WBIs of Np-O bonds at the BP86/ZORA/TZ2P level of theory.

Table S5. Calculated NBO compositions of the Np-O bonds at the BP86/ZORA/TZ2P level of theory.

References 15

S1. Experimental Procedures

Materials.

Caution! Specialized facilities and procedures are needed for this work owing to α and γ emission from ^{237}Np or α emission from natural uranium. All chemicals were reagent grade or higher and used as received. The stock solution of U(VI) in perchloric acid was prepared by dissolving $UO_2(NO_3)_2 \cdot 6H_2O$ in 1 M $HClO_4$, and the stock solutions of $^{237}Np^V$ in perchloric acid were prepared as described previously.[4] The concentration of Np(V) was determined by the absorbance at 980.2 nm (ε = 395 M^{-1} cm-1), and the concentration of perchloric acid in the stock solution was determined by Gran's titration.[5] CB[6] was synthesized from glycoluril and paraformaldehyde in HCl aqueous solution according to the reported procedure.[1] 1,1'-(hexane-1,6-diyl)bis(4-(ethoxycarbonyl)pyridine-1-ium) bromide ([C6BPCEt]Br_2)[2] and the corresponding pseudorotaxane precursor [C6BPCEt@CB6]Br_2 (**L'**-Br_2)[3] were synthesized according to the procedures reported previously.

General Methods.

^{1}H-NMR spectra were recorded on a Bruker AVANCE III (500 MHz, Bruker, Switzerland) with deuterium oxide (D_2O) as a solvent. ESI-MS spectra were obtained with a Bruker AmaZon SL ion trap mass spectrometer (Bruker, USA). UV−vis-NIR data were acquired from single crystals using a Craic Technologies microspectrophotometer. Crystals were placed on quartz slides under Krytox oil, and the data were collected from 300 to 1400 nm.

Synthesis.

NRCP-1 ([$(NpO_2)(H_2O)$(**L**)$_{0.5}$(**L**)$_{0.5}$]$(ClO_4)\cdot H_2O$): 0.05 M stock solution of $NpO_2(ClO_4)$ in 1 M $HClO_4$ (50 μL, 0.0025 mmol) were added to a suspension of the pseudorotaxane ligand of **L'**-Br_2 (4 mg, 0.0026 mmol) in water (0.8 mL) in a stainless-steel bomb, followed by adding 25 μL of 1M NaOH solution and $K_2C_2O_4$ (0.9 mg, 0.0050 mmol). The mixture was sealed, kept at 150°C for 48 h and gradually cooled to room temperature to afford several bunches of yellow-green block crystals of **NRCP-1** accompanied by a certain amount of colorless crystals of pseudorotaxane carboxylic acid, H_2**L**-ClO_4-1.

H_2**L**-ClO_4-1 ($(H_2$**L**$)_{0.5}(ClO_4)\cdot 3H_2O$): H_2**L**-ClO_4-1 was obtained as a byproduct when synthesizing the crystals of **NRCP-1** as described above.

H_2**L**-ClO_4-2 ($(H_2$**L**$)_{0.5}(H_2$**L**$)(H_2$**L**$)_{0.5}(ClO_4)_4\cdot 14H_2O$): When starting with a mixture of 0.05 M stock solution of $NpO_2(ClO_4)$ in 1 M $HClO_4$ (50 μL, 0.0025 mmol) and a suspension of the pseudorotaxane ligand of **L'**-Br_2 (4 mg, 0.0026 mmol) in water (0.8 mL), only a small amount of colorless crystals of another pseudorotaxane

carboxylic acid, H_2**L**-ClO_4-2, are produced.

UP-107 ([(UO_2)(**L**)(**L**)$_3$]$(ClO_4)_2$): 0.05 M stock solution of $UO_2(NO_3)_2$ in 1 M $HClO_4$ (50 μL, 0.0025 mmol) were added to a suspension of the pseudorotaxane ligand of **L'**-Br_2 (4 mg, 0.0026 mmol) in water (0.8 mL) in a stainless-steel bomb. The mixture was sealed, kept at 150°C for 48 h and gradually cooled to room temperature to afford light-yellow cubic crystals of **UP-107** as well as a small amount of another pseudorotaxane carboxylic acid, H_2**L**-ClO_4-2.

X-ray Single Structural Determination.

All crystals were mounted on CryoLoops with Krytox oil and optically aligned on a Bruker APEXII X-ray diffractometer equipped with a CMOS PHOTON 100 detector with a Mo Kα X-ray source (Kα = 0.71073 Å) (for **NRCP-1 and UP-107**) or a Cu Kα X-ray source (Kα = 1.54178 Å) (for H_2**L**-ClO_4-1 and H_2**L**-ClO_4-2). For all the data sets, standard APEXII software was used for determination of the unit cells and data collection control. All data was integrated using the SAINT software package, and an absorption correction was applied using SADABS. Using Olex2,[6] all crystal structures were solved by means of direct methods (SHELXS-97[7]) and refined with full-matrix least squares on SHELXL-2014.[7-8] The aromatic and hydroxyl hydrogen atoms were placed in calculated, ideal positions and refined as riding on their respective carbon or oxygen atoms. PLATON/SQUEEZE[9] was used for **NRCP-1** and **UP-107** to afford a neo-site diffraction intensities of solvent water molecules. The crystal data of these four compounds are given in Table S1 as followed. Crystallographic data for the structures in this paper have been deposited with the Cambridge Crystallographic Data Centre as supplementary publication nos. CCDC-1845094 (**NRCP-1**), CCDC-1845095 (**UP-107**), CCDC-1845096 (H_2**L**-ClO_4-1), CCDC-1845097 (H_2**L**-ClO_4-2).

Computational details

The density functional theory (DFT) calculations were carried out with the B3LYP hybrid functional[10] by using the Gaussian 09 program.[11] The structure of Np-RCP obtained from the X-ray crystal was optimized to explore the electronic properties. To maintain the state of the crystal and take into account both accuracy and efficiency of theoretical simulation, two carbon atoms, C1 and C2, in the pyridine ring were fixed in the optimization. The quasi-relativistic pseudo-potential ECP60MWB_SEG[12] and associated ECP60MWB_SEG valence basis set[13] was used to describe for Np atom, the 6-31G(d) basis set was used for the other light atoms H, C, N and O. To assess the bonding nature of Np-O bonds, natural population analysis (NPA) was

performed by using NBO 6.0 program[14] as implemented in the Amsterdam density functional (ADF 2013.01) package.[15] In NBO calculations, BP86 method and the Slater type orbital (STO) basis set TZ2P (triple-zeta with 2 polarization functions) were used,[16] without the frozen core. The scalar relativistic (SR) effects were taken into account using the zero-order regular approximation (ZORA) approach.[17] The molecular orbitals (MOs), natural bonding orbitals, Nalewajski-Mrozek (NM) valence indices[18] and Wiberg bond indices (WBIs)[19] of Np-O bonds were obtained based on the calculations of ADF. The topological analysis was carried out using the quantum theory of atoms in molecules (QTAIM)[20] with the Multiwfn program.[21]

S2. Figures and Tables

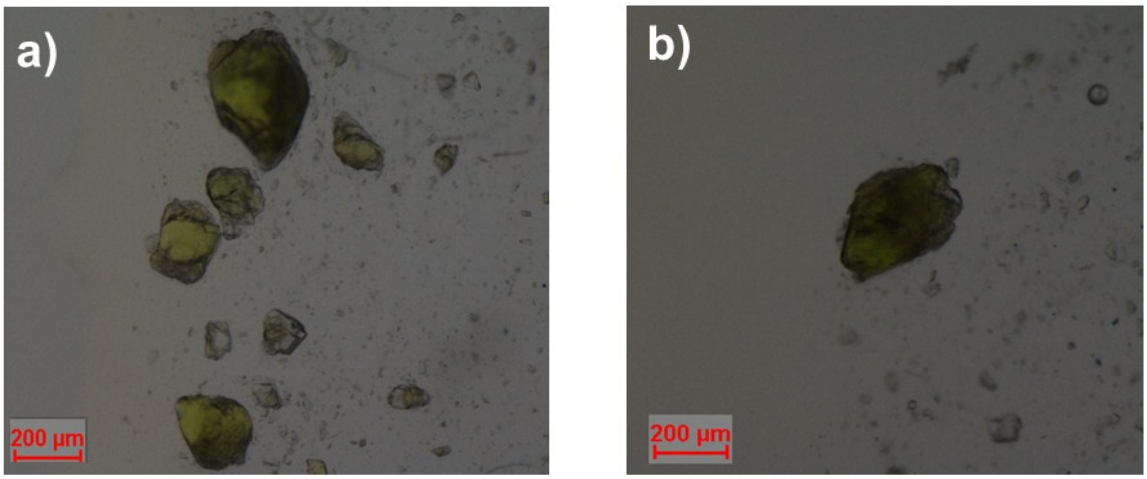

Figure S1. Optical photograph of yellow-green block crystals of **NRCP-1**: a) yellow-green block crystals for **NRCP-1**, accompanied by a certain amount of colorless crystals for pseudorotaxane carboxylic acid, H_2**L**-ClO_4-1; b) a snapsnot of **NRCP-1**.

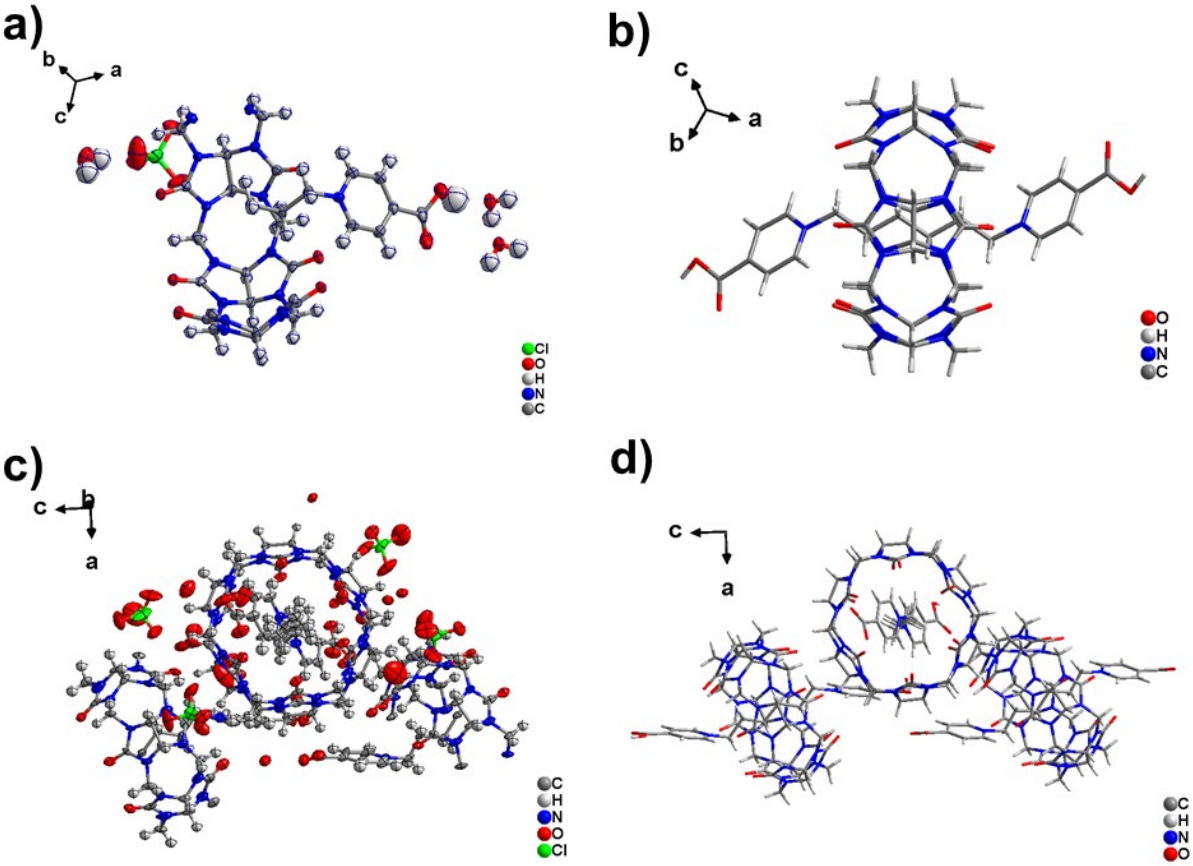

Figure S2. Crystal structures of H_2**L**-ClO_4-1 (a) and H_2**L**-ClO_4-2 (b).

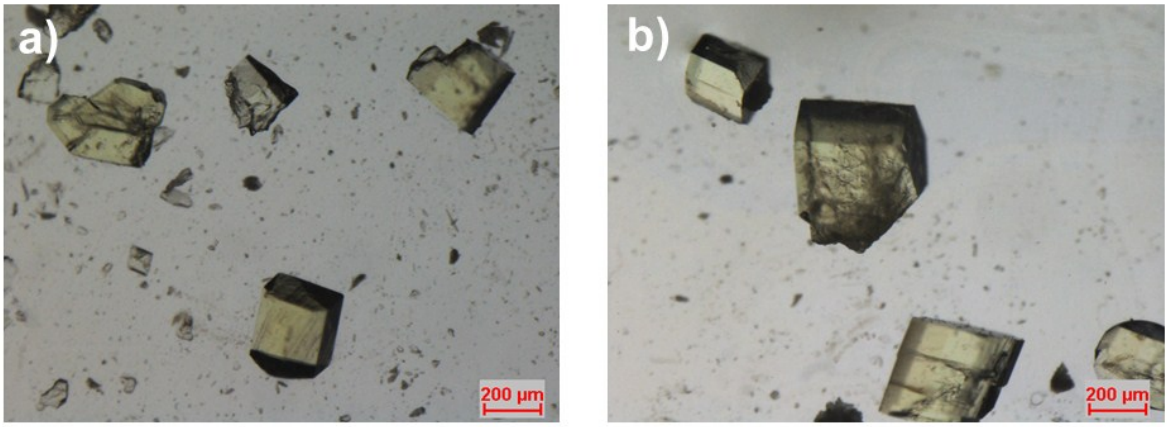

Figure S3. Optical photograph of light-yellow block crystals of **UP-107**: a) light-yellow cubic crystals of **UP-107**, accompanied by a certain amount of colorless crystals for pseudorotaxane carboxylic acid, H_2**L**-ClO_4-2; b) a snapsnot of **UP-107**.

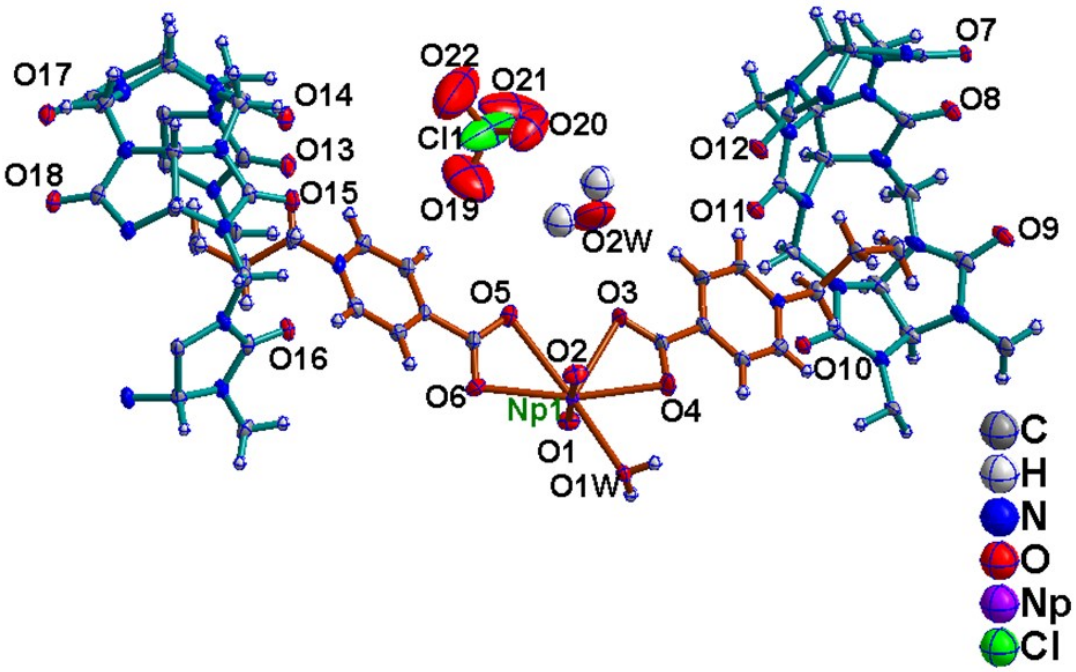

Figure S4. The asymmetric unit of **NRCP-1** containing one neptunyl ion, two halves of C6BPCA@CB6 pseudorotaxane ligands, and one coordinated water molecule as well as one crystal lattice water molecule and one perchlorate counter-ion

.

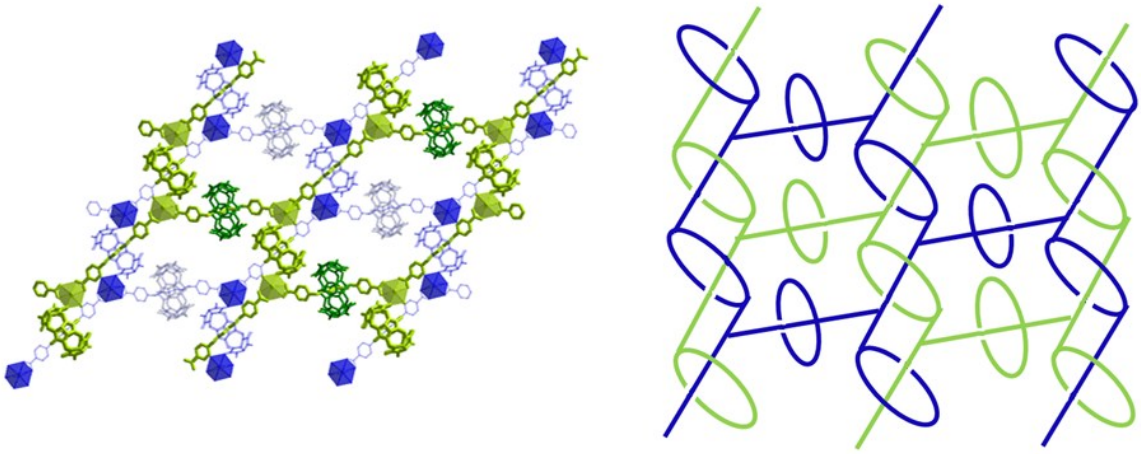

Figure S5. A unique interwoven neptunium(V)-rotaxane coordination network of **NRCP-1** with two sets of independent but mechanically-interlocked neptunyl-rotaxane layered structures.

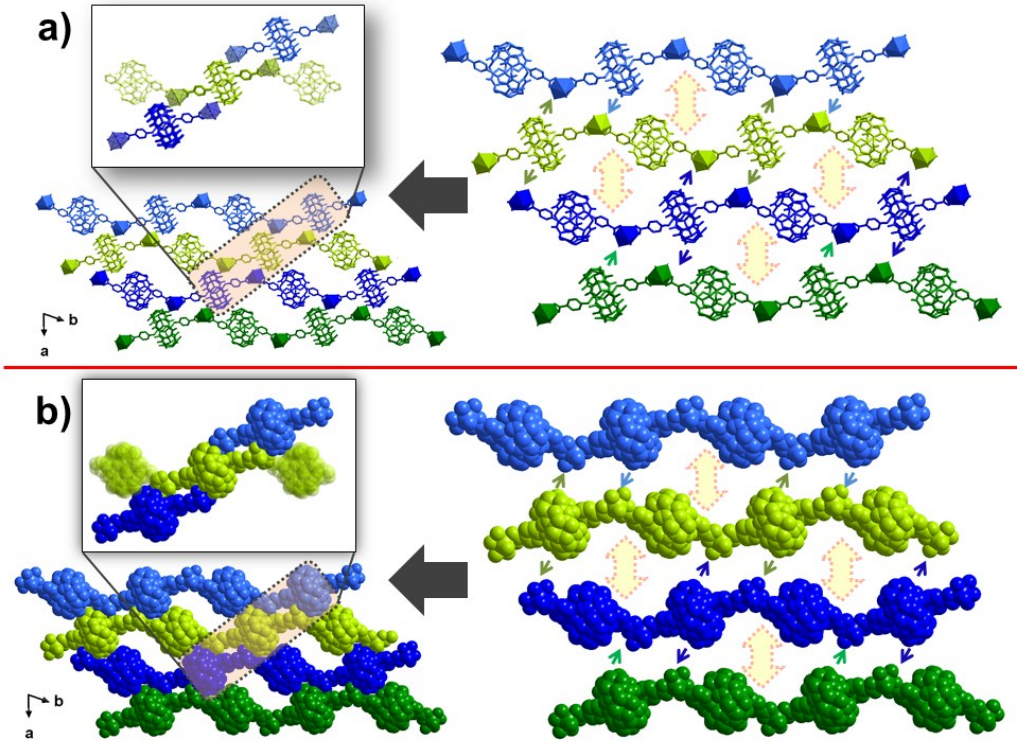

Figure S6. The interwoven neptunium(V)-rotaxane coordination network of **NRCP-1** separated into an array of neptunyl-rotaxane one-dimensional chain cross-linked through coordination of exposed carbonyl groups of CB6 coordinating with neptunyl centers from adjacent chains in stick model (a) and space-filling model (b).

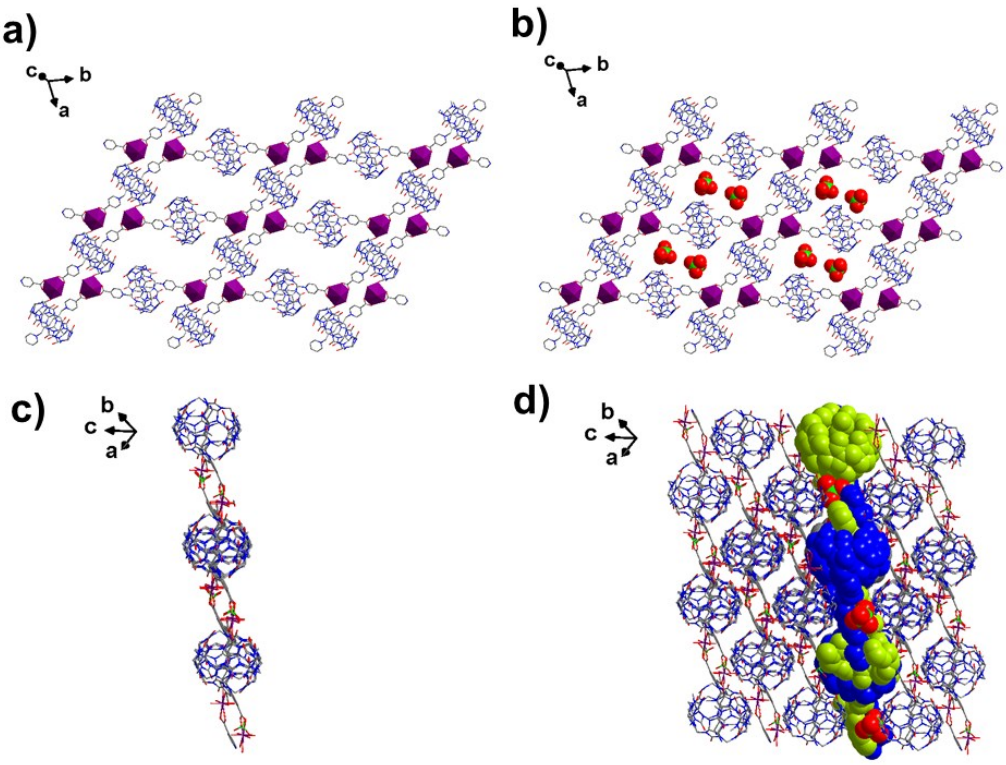

Figure S7. a) Interwoven coordination network; b) Interwoven coordination network with all the perchlorate anions fill in pairs in the quadrilateral holes; c) interwoven coordination network viewed from the side-on; d) closely packing of coordination networks in crystal lattice through weak interactions.

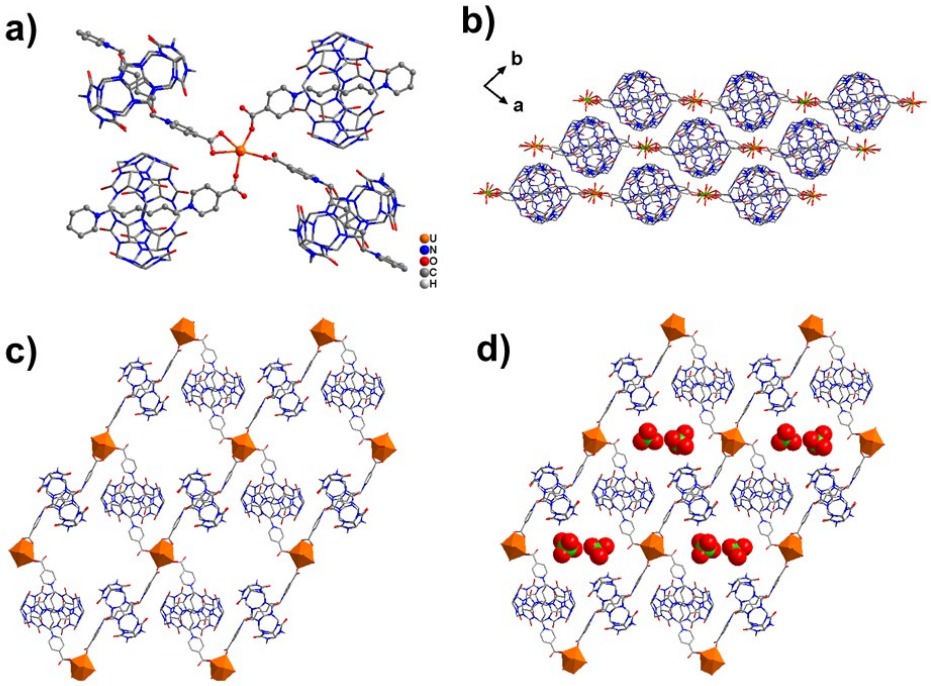

Figure S8. a) The crystallographically unique uranyl center with a pentagonal-bipyramid geometry in **UP-107**; b) crystal packing of two-dimensional networks in **UP-107**; c) a two-dimensional polyrotaxane network with rhombic-shaped loops in **UP-107**; d) perchlorate ions in pair trapped in the rhombic-shaped cavity of two-dimensional polyrotaxane network in **UP-107**.

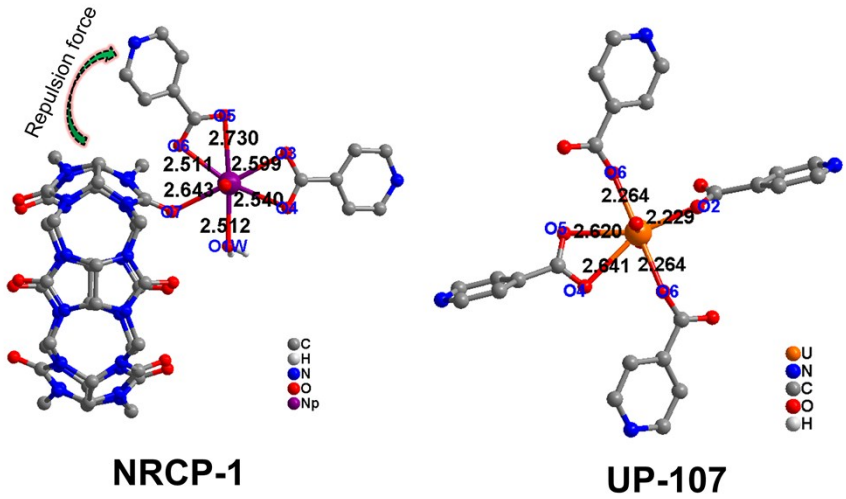

Figure S9. A direct comparison of bond distances between metal ion and oxygen donors in **NRCP-1** (left) and **UP-107** (right).

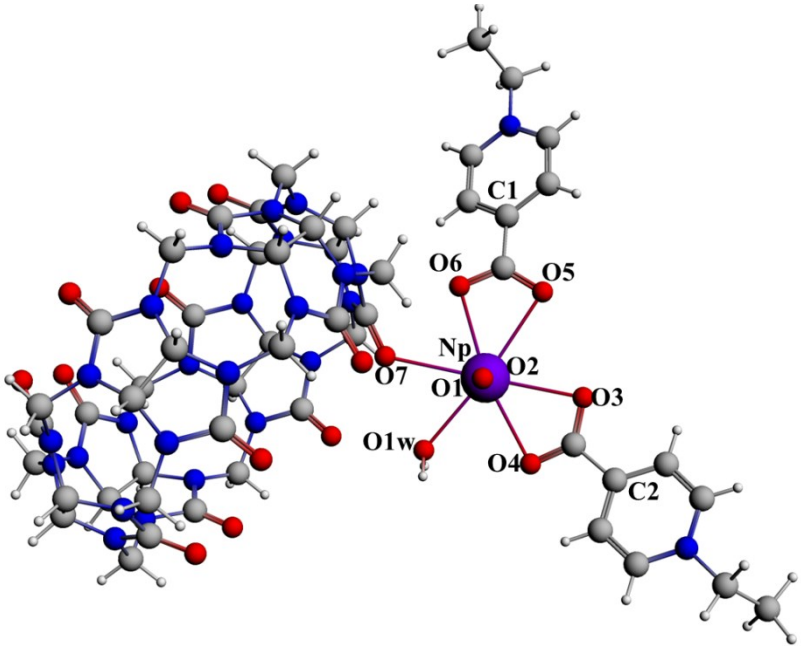

Figure S10. The simplified model of coordination sphere of neptunyl derived from crystal structure of **NRCP-1**.

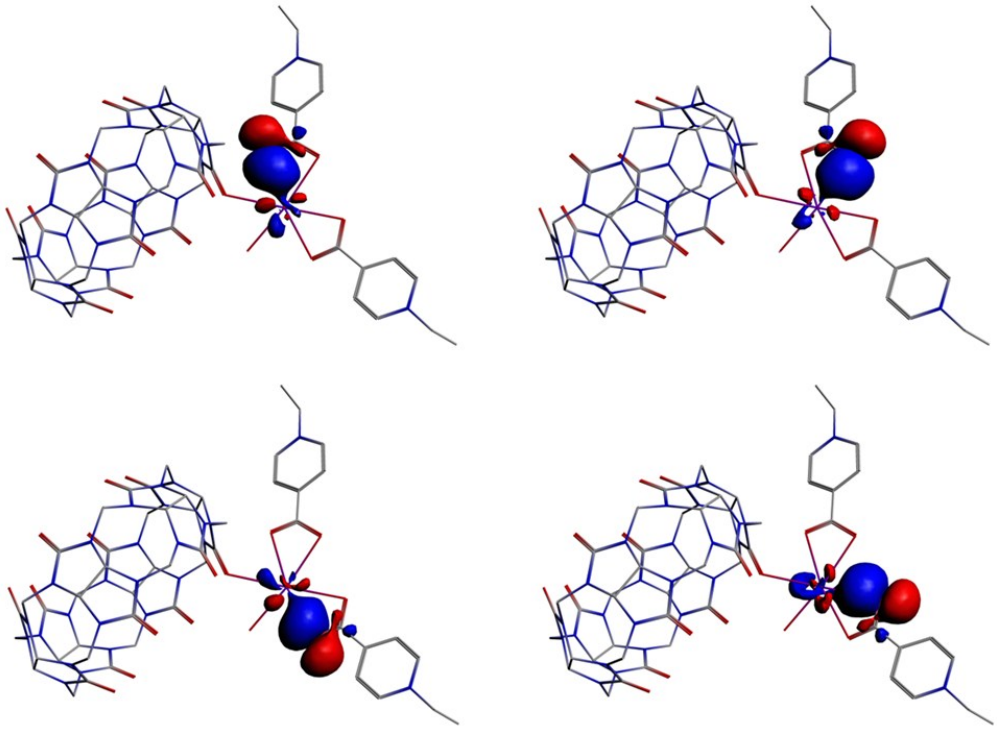

Figure S11. Natural bond orbitals of Np-O bonds. The isosurface value of the MOs is established as 0.03 au.

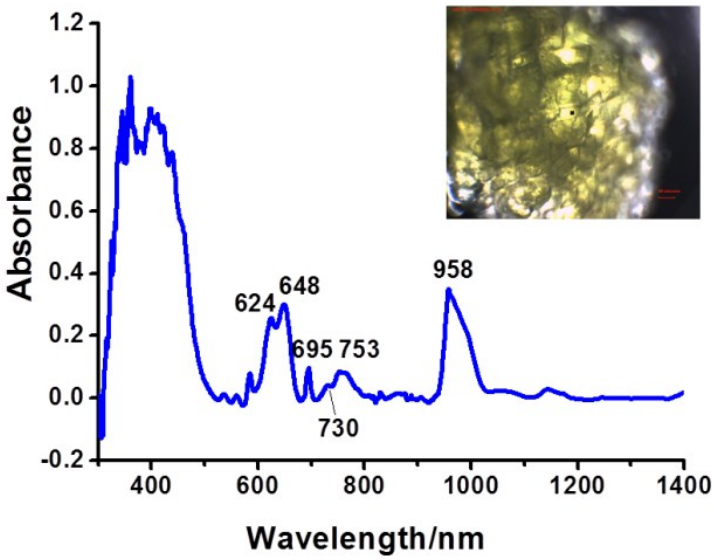

Figure S12. The UV-vis-NIR absorption spectroscopy recorded from crystals of **NRCP-1** using a microspectrophotometer. Insert: optical photograph of yellow-green block crystals of **NRCP-1**.

Table S1. Crystal data and structure refinement for **NRCP-1**, **UP-107**, H_2**L**-ClO_4-1 and H_2**L**-ClO_4-2.

	NRCP-1	**UP-107**	H_2**L**-ClO_4-1	H_2**L**-ClO_4-2
formula	$C_{54}H_{60}ClN_{26}NpO_{24}$	$C_{108}H_{112}Cl_2N_{52}O_{42}U$	$C_{54}H_{70}Cl_2N_{26}O_{30}$	$C_{108}H_{114}Cl_4N_{52}O_{62}$
formula weight	1729.73	3119.42	1634.26	3274.31
crystal system	triclinic	triclinic	triclinic	triclinic
space group	$P\bar{1}$	$P\bar{1}$	$P\bar{1}$	$P\bar{1}$
a, Å	15.2162(9)	12.7487(6)	12.1092(6)	12.6870(12)
b, Å	15.3864(9)	15.3678(7)	12.2000(7)	15.9445(15)
c, Å	15.6650(9)	17.1021(8)	12.8040(7)	35.622(3)
α, deg	73.052(2)	90.328(2)	106.917(4)	86.375(5)
β, deg	82.550(2)	97.214(2)	112.567(4)	88.628(5)
γ, deg	67.868(2)	95.183(2)	92.559(4)	67.119(4)
V, Å^3	3248.9(3)	3310.0(3)	1644.78(16)	6625.7(11)
Z	2	1	1	2
T, K	170	170	170	170
Dc, g/cm^3	1.768	1.565	1.650	1.641
***μ* (mm^{-1})**	1.744[a]	1.370[b]	1.885[c]	1.889[d]
F(000)	1736	1586	850	3380
Theta(Min, Max) [Deg]	2.916, 27.583	2.939, 27.548	3.848, 68.588	3.192, 58.447
R_{int}	0.0391	0.0335	0.1108	0.0678
Goodness-of-fit (S)	1.061	1.030	1.017	1.124
R_1, *w*R_2 [I ≥ 2σ(I)]	0.0334, 0.0879	0.0447, 0.1228	0.0666, 0.1327	0.1290, 0.3611
R_1, *w*R_2 (all data)	0.0395, 0.0911	0.0471, 0.1252	0.1368, 0.1600	0.2023, 0.4344

[a, b]: Mo K_α (λ = 0.71073 Å); [c, d]: Cu K_α (λ = 1.54178 Å).

Table S2. Selected bond distances (Å) related to neptunium center in **NRCP-1** and **UP-107**.

		NRCP-1	
Np(1)-O(1)	1.818(2)	Np(1)-O(2)	1.812(3)
Np(1)-O(3)	2.599(3)	Np(1)-O(4)	2.540(3)
Np(1)-O(5)	2.730(3)	Np(1)-O(6)	2.511(3)
Np(1)-O(7)	2.643(2)	Np(1)-O(1W)	2.512(2)
O(1)-Np(1)-O(2)	179.68(13)		
		UP-107	
U(1)-O(1)	1.738(4)	U(1)-O(2)	2.229(7)
U(1)-O(4)	2.641(6)	U(1)-O(5)	2.620(8)
U(1)-O(6)	2.264(4)		
O(1)-U(1)-O(1')	180.0		

Table S3. Products under synthesis conditions from uranium or neptunium sources.

Metal source	Initial aqueous solution [a]	Initial aqueous solution + 25 μL NaOH (1M) + 5 μmoL $K_2C_2O_4$
UO_2^{2+}	**UP-107** H_2**L**-ClO_4-2	-
NpO_2^{+}	H_2**L**-ClO_4-2	**NRCP-1** H_2**L**-ClO_4-1

[a] Reaction components of initial aqueous solution: C6BPCEt@CB6, 4 mg; NpO_2^{+} OR UO_2^{2+} (50 mmol in 1M $HClO_4$), 50 μL; pure H_2O, 800 μL.

Table S4. Calculated Np-O bond distances (Å) and the electron density (ρ(r), au), and Laplacian ($\nabla^2\rho$(r), au) at the Np-O BCP at the B3LYP/ECP60MWB/6-31G(d) level of theory, and the NM and WBIs of Np-O bonds at the BP86/ZORA/TZ2P level of theory.

	Expt.	Cal.	NM	WBIs	ρ(r)	$\nabla^2\rho$(r)
Np-O1	1.818	1.784	2.801	2.142	0.276	0.252
Np-O2	1.812	1.803	2.718	2.066	0.273	0.264
Np-O1W	2.512	2.548	0.493	0.344	0.044	0.191
Np-O3	2.599	2.658	0.404	0.300	0.031	0.117
Np-O4	2.540	2.603	0.445	0.326	0.038	0.144
Np-O5	2.730	2.684	0.403	0.292	0.047	0.183
Np-O6	2.511	2.622	0.449	0.328	0.028	0.112
Np-O7	2.643	2.561	0.414	0.309	0.045	0.172

Table S5. Calculated NBO compositions of the Np-O bonds at the BP86/ZORA/TZ2P level of theory.

Np-O	Np%	O%	Contributions of Np AOs (%)	Contributions of O AOs (%)
Np-O3	8.82	91.18	7s(10.94) 6d(48.72) 5f(40.16)	2s(14.30)2p(85.56)
Np-O4	8.71	91.29	7s(12.90) 6d(47.90%) 5f(39.01)	2s(13.08)2p(86.76)
Np-O5	8.44	91.56	7s(23.14) 6d(50.59) 5f(25.99)	2s(11.16)2p(88.66)
Np-O6	7.09	92.91	7s(24.69) 6d (52.83) 5f (22.15)	2s(8.77)2p(91.04)

References

[1] L. Rao, T. G. Srinivasan, A. Yu. Garnov, Zanonato, P.; P. Di Bernardo, A. Bismondo, *Geochim. Cosmochim. Acta,* **2004**, *68*, 4821-4830.

[2] G. Gran, *Analyst* **1952**, *77*, 661-671.

[3] A. Day, A. P. Arnold, R. J. Blanch, B. Snushall, *J. Org. Chem.*, **2001**, *66*, 8094-8100.

[4] a) F. H. Huang, C. Slebodnick, E. J. Mahan, H.W. Gibson, *Tetrahedron,* **2007**, *63*, 2875-2881; b) X. Z. Sun, B. Li, C. L. Xia, X. H. Zhou, H.B. Zhang, *CrystEngComm*, **2012**, *14*, 8525-8529.

[5] a) L. Mei, L. Wang, L. Y. Yuan, S. W. An, Y. L. Zhao, Z. F. Chai, P. C. Burns, W. Q. Shi, *Chem. Commun.,* **2015**, *51*, 11990-11993.; b) L. Mei,; Q. Y., Wu,; C. M. Liu,; Y. L. Zhao,; Z. F. Chai,; W. Q. Shi, , *Chem. Commun.,* **2014**, *50*, 3612-3615.

[6] O. V. Dolomanov, L. J. Bourhis, R. J. Gildea, J. A. K. Howard, H. Puschmann, *J Appl. Crystallogr.* **2009**, *42*, 339-341.

[7] G. M. Sheldrick, *Acta Crystallogr. A*, **2008**, *64*, 112-122.

[8] G. M. Sheldrick, *Acta Crystallogr. A,* **2015**, *71*, 3-8.

[9] A. L. Spek, *Acta Crystallogr. C* **2015**, *71*, 9-18.

[10] a) C. T. Lee, W. T. Yang, R. G. Parr, Development of the Colle-salvetti Correlation-Energy Formula into a Functional of the Electron-Density. *Phys. Rev. B* **1988,** *37*, 785-789; b) Becke, A. D. Density-Functional Exchange-Energy Approximation with Correct Asymptotic-Behavior. *Phys. Rev. A* **1988,** *38*, 3098-3100.

[11] M. J. Frisch, G. W. Trucks, H. B. Schlegel, G. E. Scuseria, M. A.Robb, J. R. Cheeseman, G. Scalmani, V. Barone, B. Mennucci, G. A. Petersson, H. Nakatsuji, M. Caricato, X. Li, H. P. Hratchian, A. F. Izmaylov, J. Bloino, G. Zheng, J. L. Sonnenberg, M. Hada, M. Ehara, K. Toyota, R. Fukuda, J. Hasegawa, M. Ishida, T. Nakajima, Y. Honda, O. Kitao, H. Nakai, T. Vreven, J. A. Montgomery Jr., J. E. Peralta, F. Ogliaro, M. J. Bearpark, J. Heyd, E. N. Brothers, K. N. Kudin, V. N. Staroverov, R. Kobayashi, J. Normand, K. Raghavachari, A. P. Rendell, J. C. Burant, S. S. Iyengar, J. Tomasi, M. Cossi, N. Rega, N. J. Millam, M. Klene, J. E. Knox, J. B. Cross, V. Bakken, C. Adamo, J. Jaramillo, R. Gomperts, R. E. Stratmann, O. Yazyev, A. J. Austin, R. Cammi, C. Pomelli, J. W. Ochterski, R. L. Martin, K. Morokuma, V. G. Zakrzewski, G. A. Voth, P. Salvador, J. J. Dannenberg, S. Dapprich, A. D. Daniels, Ö. Farkas, J. B. Foresman, J. V. Ortiz, J. Cioslowski, D. J. Fox, *Gaussian 09*, Gaussian, Inc.: Wallingford, CT, USA, 2009.

[12] X. Cao, M. Dolg, H. Stoll, Valence Basis sets for Relativistic Energy-Consistent Small-Core Actinide pseudopotentials. *J. Chem. Phys.* **2003,** *118*, 487-496.

[13] X. Cao, M. Dolg, Segmented Contraction Scheme for Small-Core Actinide Pseudopotential Basis Sets. *J. Mol. Struct. (THEOCHEM)* **2004,** *673*, 203-209.

[14] E. D. Glendening, J. K. B., A. E. Reed, J. E. Carpenter, J. A. Bohmann, C. M. Morales, C. R. Landis, and F. Weinhold NBO 6.0. http://nbo6.chem.wisc.edu/

[15] a) C. Fonseca Guerra, J. G. Snijders, G. te Velde, E. J. Baerends, Towards an order-N DFT method. *Theor. Chem. Acc.* **1998,** *99*, 391-403; b) G. te Velde, F. M. Bickelhaupt, E. J. Baerends, C. Fonseca Guerra, S. J. A. van Gisbergen, J. G. Snijders, T. Ziegler, Chemistry with ADF. *J. Comput. Chem.* **2001,** *22*, 931-967.

[16] E. Van Lenthe, E. J. Baerends, Optimized Slater-type basis sets for the elements 1–118. *J. Comput. Chem.* **2003,** *24*, 1142-1156.

[17] E. Van Lenthe,, E. J. Baerends, J. G. Snijders, Relativistic regular two‐component Hamiltonians. *J. Chem. Phys.* **1993,** *99*, 4597-4610.

[18] a) R. F. Nalewajski, J. Mrozek, Modified valence indices from the two-particle density matrix. *Int. J. Quantum Chem.* **1994,** *51*, 187-200; b) R. F. Nalewajski, J. Mrozek, A. Michalak, Two-electron valence indices from the Kohn-Sham orbitals. *Int. J. Quantum Chem.* **1997,** *61*, 589-601.

[19] K. B. Wiberg, Application of the pople-santry-segal CNDO method to the cyclopropylcarbinyl and cyclobutyl cation and to bicyclobutane. *Tetrahedron* **1968,** *24*, 1083-1096.

[20] R. F. W. Bader, *Atoms in Molecules: A Quantum Theory*. OUP: Oxford, U.K., 1990.

[21] T. Lu, F. Chen, Multiwfn: A Multifunctional Wavefunction Analyzer. *J. Comput. Chem.* **2012,** *33*, 580-592.